Rock Mech Rock Eng (2016) 49:3371–3376
DOI 10.1007/s00603-016-0928-x

TECHNICAL NOTE

Truncated Gaussian Simulation to Map the Spatial Heterogeneity of Rock Mass Rating

Marisa Pinheiro[1] · Xavier Emery[2,3] · Tiago Miranda[1] · Javier Vallejos[2,3]

Received: 30 March 2015 / Accepted: 8 February 2016 / Published online: 20 February 2016

Keywords Rock mass rating · Rock mechanics · Geostatistical simulation · Spatial heterogeneity · Spatialuncertainty

1 Introduction

Mapping the intrinsic spatial variability of rock mass characteristics is an essential issue in geotechnical and geomechanical engineering, as these characteristics have a significant impact on the behavior of underground structures. Such mapping can be performed by recurrence of geostatistical models, in which the geomechanical parameters are viewed as outcomes (realizations) of spatial random fields whose properties can be inferred from the available in situ measurements and laboratory tests. In this context, several authors already applied geostatistics to predict or simulate characteristics such as lithofacies (Rosenbaum et al. 1997), rock quality designation (RQD) (Madani and Asghari 2013; Ozturk and Simdi 2014; Ozturk 2002), rock mass rating (RMR) (Ryu et al. 2003; Seokhoom et al. 2004; Stavropoulou et al. 2007; Exadaktylos and Stavropoulou 2008; Jeon et al. 2009; Egaña and Ortiz 2013) and geological strength index (GSI) (Ozturk and Simdi 2014; Deisman et al. 2013).

✉ Marisa Pinheiro
marisamotapinheiro@gmail.com

[1] ISISE, University of Minho, Azurém, 4800-058 Guimarães, Portugal

[2] Department of Mining Engineering, University of Chile, Avenida Tupper 2069, Santiago, Chile

[3] Advanced Mining Technology Center, University of Chile, Avenida Beauchef 850, Santiago, Chile

In this work, the RMR system is used to geomechanically characterize the rock mass. This empirical approach allows classifying the rock mass by a value varying from 0 to 100, obtained by summing the weights attributed to six parameters (Bieniawski 1989):

- P1—uniaxial compressive strength (UCS) of rock material;
- P2—rock quality designation (RQD), measured along the direction of greater fracture frequency;
- P3—spacing of discontinuities (FF), measured along the direction of greater fracture frequency;
- P4—condition of discontinuities;
- P5—groundwater conditions;
- P6—orientation of discontinuities.

However, the RMR under consideration here is the so-called basic RMR, which is obtained by accounting only for the first five parameters. To map this basic RMR, in this paper we propose to individually simulate parameters P1–P5 and subsequently sum them to obtain the final RMR value. A novelty of this approach with respect to existing literature (Egaña and Ortiz 2013) is that the RMR is simulated through its underlying parameters and that these parameters are modeled as random fields measured on a discrete quantitative scale, as they only assume integer values, using a specific geostatistical model (the so-called truncated Gaussian model). The purpose of detailing the five parameters is to obtain further information about the rock mass characteristics and facilitate an overall view of the most important parameters, i.e., the ones that most contribute to the RMR (parameters with the highest simulated values) or the ones that are most responsible for the uncertainty in the unknown RMR at unsampled locations (parameters with a wide range of simulated values at a given location are more significant for the uncertainty in

the RMR than parameters with a narrow range of simulated values). The model is implemented using real data and validated using the split-sample technique.

2 Truncated Gaussian Simulation

The truncated Gaussian model (Armstrong et al. 2011) allows simulating a random field with discrete values through the truncation of a second-order stationary Gaussian random field. The model is specified by one or more truncation thresholds and by the covariance function or the variogram of the Gaussian random field. In practice, the thresholds are defined to reproduce the experimental proportion of each class of discrete values, while the variogram is inferred on the basis of its relationship with the class-indicator variograms (Emery and Cornejo 2010).

The discrete-valued random field can be simulated and conditioned to a set of available data through the following steps:

1. The Gaussian random field is simulated first at the data locations, using an iterative algorithm known as the Gibbs sampler (Armstrong et al. 2011; Lantuéjoul 2002).
2. The Gaussian random field is then simulated at the target locations, conditionally to the Gaussian values obtained at the previous step. At this stage, the turning bands algorithm (Lantuéjoul 2002) is used.
3. The simulated Gaussian field is truncated back into a discrete-valued random field.

3 Case study

Truncated Gaussian simulation was applied to a case study to map the RMR in an epithermal gold deposit located in the Cordillera de Los Andes, region of Atacama, northern Chile, and surveyed through a set of exploration boreholes. The regional geology of the area is characterized by a group of intrusive, volcanic and sedimentary rocks, affected by fault zones that control the mineralization.

The available data comprised 3969 samples obtained from boreholes with lengths ranging from 96 to 390 m. According to the results of rock mechanics laboratory tests and the RMR values obtained from the borehole samples, the rock mass is classified with a quality of regular to good (RMR values mostly in the range of 50–60). Concerning the individual parameters, P1 varies within a short range, meaning that the UCS of the intact rock is almost constant, unlike P2 and P3 that vary in a much wider range showing very different levels of rock mass fracturing. In contrast, the fourth parameter (P4) is equal to 20 for all the samples, so in the models it will be considered as constant in space and not simulated. This parameter is related to the condition of the discontinuities, so they are all classified as having slightly rough surfaces with a separation smaller than 1 mm and a highly weathered wall rock. Lastly, parameter P5 varies within a short range, with only two different scores, representing a groundwater condition that is mostly wet and punctually damp (Table 1).

Table 1 Statistics of experimental data

Variable	P1	P2	P3	P4	P5	RMR
Number of data	3969	3969	3969	3969	3969	3969
Minimum	12	1	5	20	7	48
Maximum	14	20	19	20	10	78
Mean	13.07	16.30	10.16	20.00	7.03	66.6
Variance	1.00	7.05	4.13	0	0.10	14.21

Table 2 Correlation matrix of experimental data

Variable	P1	P2	P3	P4	P5
P1	1	−0.096	−0.164	0.000	−0.113
P2	−0.096	1	0.292	0.000	0.045
P3	−0.164	0.292	1	0.000	−0.032
P4	0.000	0.000	0.000	1	0.000
P5	−0.113	0.045	−0.032	0.000	1

The correlation matrix of the parameters (Table 2) indicates a weak dependence between them (all the correlation coefficients are <0.3 in absolute value), meaning that the information on a parameter brings little information on the other parameters. As such, the RMR parameters can be simulated separately; joint simulation, which enhances the simulation of a set of random fields to reproduce their cross-correlation (Emery and Cornejo 2010), is not necessary in this case.

3.1 Modeling the Univariate Distributions

The data of P1 only present two different scores, 12 and 14, with relative proportions of 0.468 and 0.532, respectively. This distribution can therefore be modeled by truncating a standard normal distribution, using a single truncation threshold set to $G^{-1}(0.468) = -0.08$, where G stands for the standard normal cumulative distribution function. Likewise, the data of P5 only assume two different scores, 7 and 10, with relative proportions of 0.989 and 0.011, respectively. Again, in the model a single truncation threshold, here equal to $G^{-1}(0.989) = 2.29$, is used. In contrast, the data of P2 and P3 assume many different scores. As a result, a larger number of truncation thresholds have to be defined (Tables 3, 4).

Table 3 Calculated proportions for P2 with the corresponding Gaussian thresholds

Category	Cumulative proportion	Lower threshold	Upper threshold
1	0.0030	$-\infty$	−2.7478
2	0.0032	−2.7478	−2.7266
3	0.0033	−2.7266	−2.7164
4	0.0043	−2.7164	−2.6276
5	0.0073	−2.6276	−2.4422
6	0.0080	−2.4422	−2.4089
7	0.0150	−2.4089	−2.1701
8	0.0200	−2.1701	−2.0537
9	0.0250	−2.0537	−1.9600
10	0.0360	−1.9600	−1.7991
11	0.0510	−1.7991	−1.6352
12	0.0780	−1.6352	−1.4187
13	0.1120	−1.4187	−1.2160
14	0.1710	−1.2160	−0.9502
15	0.2710	−0.9502	−0.6098
16	0.4520	−0.6098	−0.1206
17	0.6200	−0.1206	0.3055
18	0.8180	0.3055	0.9078
19	0.9900	0.9078	2.3263
20	1.0000	2.3263	$+\infty$

Table 4 Calculated proportions for P3 with the corresponding Gaussian thresholds

Category	Cumulative proportion	Lower threshold	Upper threshold
1	0	$-\infty$	$-\infty$
2	0	$-\infty$	$-\infty$
3	0	$-\infty$	$-\infty$
4	0	$-\infty$	$-\infty$
5	0.0500	$-\infty$	−1.6449
6	0.0501	−1.6449	−1.6439
7	0.0502	−1.6439	−1.6429
8	0.1842	−1.6429	−0.8995
9	0.3432	−0.8995	−0.4037
10	0.5422	−0.4037	0.1060
11	0.8152	0.1060	0.8972
12	0.9182	0.8972	1.3931
13	0.9582	1.3931	1.7302
14	0.9762	1.7302	1.9809
15	0.9872	1.9809	2.2322
16	0.9912	2.2322	2.3739
17	0.9952	2.3739	2.5899
18	0.9998	2.5899	3.5401
19	1.0000	3.5401	$+\infty$
20	1.0000	$+\infty$	$+\infty$

3.2 Modeling Spatial Continuity: Variogram Analysis

The variograms of the Gaussian random fields to be simulated are inferred along the main directions of anisotropy, which correspond to the horizontal plane and vertical direction. These variograms are fitted using combinations of basic nested structures (exponential, spherical, cubic and Gaussian); the reader is referred to Chilès and Delfiner (2012) for the mathematical definition of these basic models. It should be noticed that none of the variograms exhibit a nugget effect (discontinuity near the origin), indicating that the underlying parameters are continuous in space. Moreover, the variogram models for P1, P3 and P5 have a smooth behavior near the origin, which reflects that the spatial variations of these parameters are very regular at a short scale, whereas parameter P2 exhibits a more irregular behavior at short scale.

3.3 Conditional Simulations Results

Truncated Gaussian simulation is performed with an adaptation of a previously published computer program (Emery 2007). The number of realizations is set to 100, so that the post-processing outputs (average and conditional probabilities) could be calculated with a reasonable approximation. The realizations are conditioned to the borehole data.

To facilitate the display, the locations targeted for simulation correspond to a regular two-dimensional grid placed at elevation 3439 m, with a mesh of 10 m × 10 m and a total of 150 nodes along both the east and north directions. The average of the 100 realizations is calculated to map the expected RMR over the region of interest (Fig. 1a). Additionally, the first realization is also mapped to demonstrate the actual spatial variability of RMR (Fig. 1b). It is worth noticing that the map of the realization average tends to blur the contrasts and that spatial heterogeneities appear as much more attenuated. Other outputs can be mapped, such as the probability that RMR exceeds or falls short of a predefined value. This representation is of great value if one wants to identify regions where very high or low geomechanical properties would be present, and with which probability. As an example, for this case, a map of the probability that the actual (unknown) RMR exceeds a threshold of 70 is shown in Fig. 1c. One can also map the standard deviation of the realizations (Fig. 1d), which reflects the level of uncertainty in the true value of RMR: the higher uncertainty occurs in regions with higher variability or with fewer boreholes, especially the northwestern region for which one observes strong contrasts in the mapped RMR values (Fig. 1a) and a lack of sampling information.

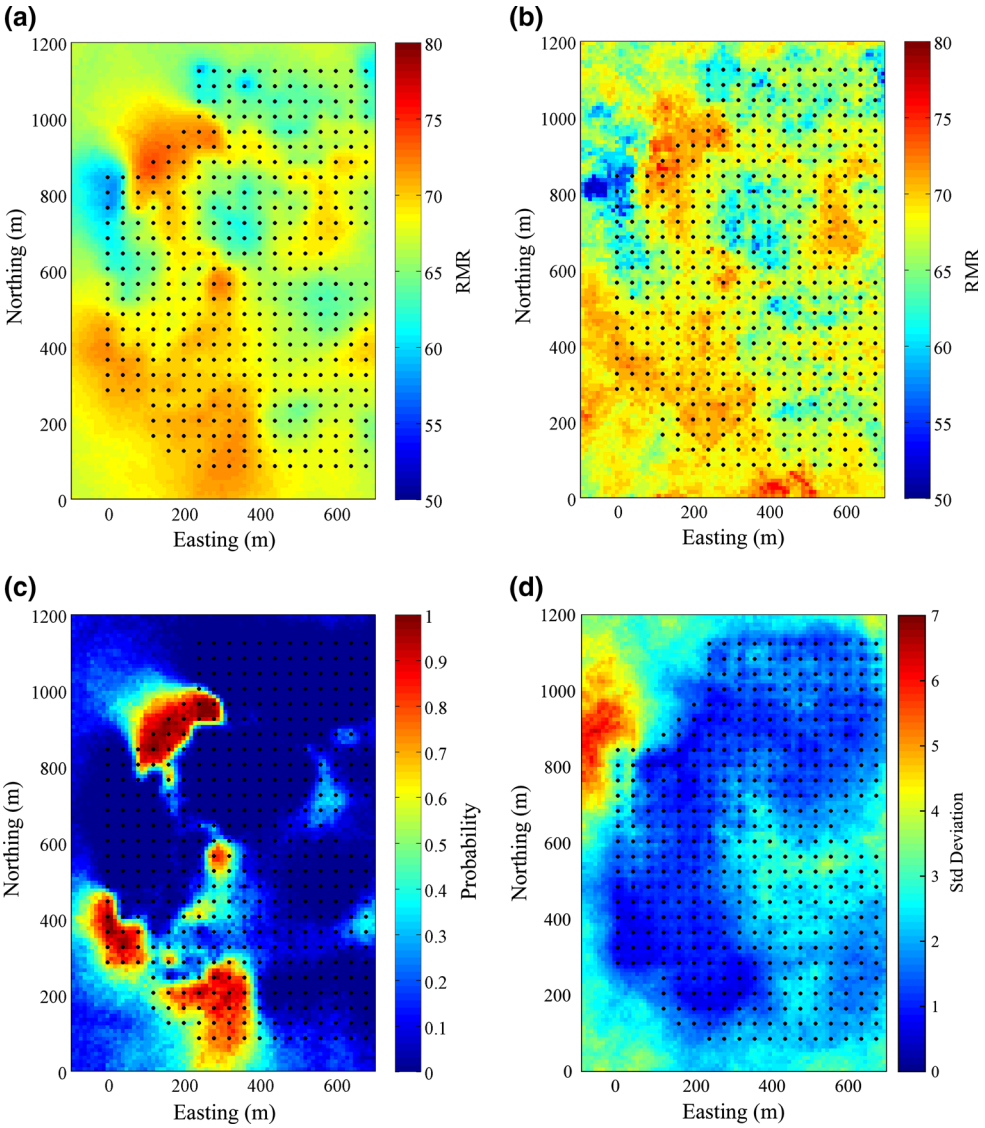

Fig. 1 Maps of RMR at elevation 3439 m, for: **a** average of 100 realizations; **b** realization no. 1; **c** probability that RMR exceeds a threshold of 70; **d** standard deviation of 100 realizations. Data locations have been superimposed

Figure 2 shows the maps of P1, P2 and P3 for the first realization, which help to visualize the variability of the intact rock strength and joints spatial distribution in the rock mass. The individual analysis of fracturation parameters can, by itself, result in a powerful tool in underground works to understand the regions where the rock mass can be more or less fractured.

3.4 Split-Sample Validation

To validate the simulation model, the original data set is randomly divided into two subsets, each containing one half of the data. The first subset (training subset) is then used to simulate the underlying RMR parameters at the locations of the data belonging to the second subset (validation subset). Two types of validations are performed, aimed at assessing the prediction capability and the modeling uncertainty.

First, the prediction capability compares the expected RMR, calculated as the average over 100 realizations of the underlying parameters sum, with the actual values at the locations of the validation subset. The coefficient of determination (R^2) between the expected and real RMR values is calculated, resulting in a value of 0.74. This indicates that the simulation allows a reasonably accurate prediction of RMR (Fig. 3a). Accuracy is confirmed by calculating the root mean-squared error (RMSE) of the expected values. The RMSE value is 1.88 and, considering that the RMR varies from 0 to 100, an error less than 2 is almost residual.

With respect to uncertainty modeling, the validation consists of a so-called accuracy plot (Goovaerts 2001). In this plot, one considers a given probability p and, based on the obtained realizations, defines at each target location an interval with such a probability. Subsequently, the location is assigned a value of 1 if the true data belongs to the

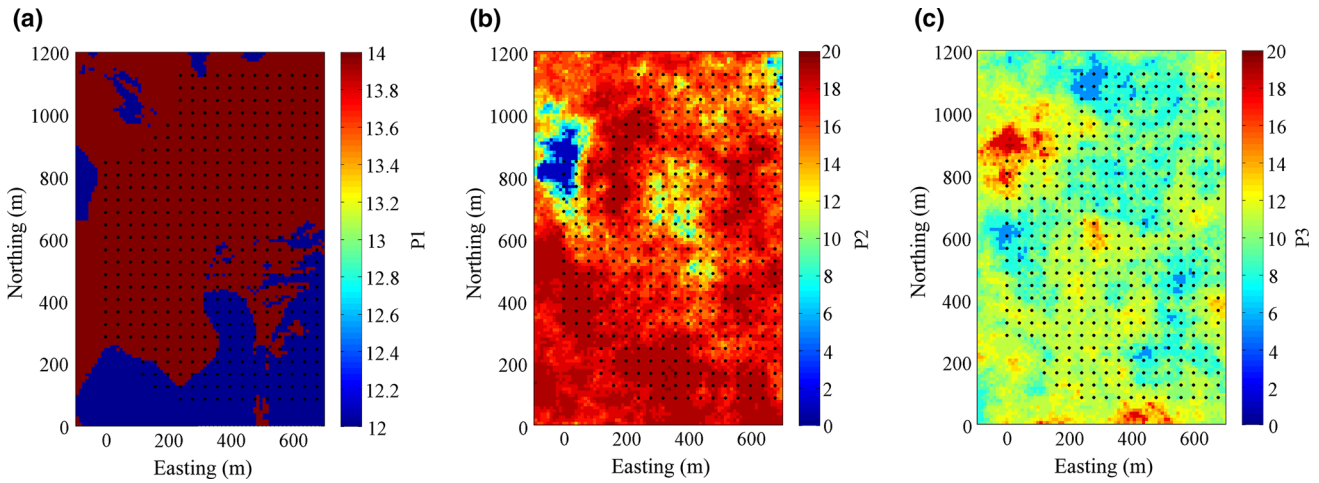

Fig. 2 Maps of first three parameters for realization no 1 at elevation 3439 m: **a** parameter 1 (UCS); **b** parameter 2 (RQD); **c** parameter 3 (FF). Data locations have been superimposed

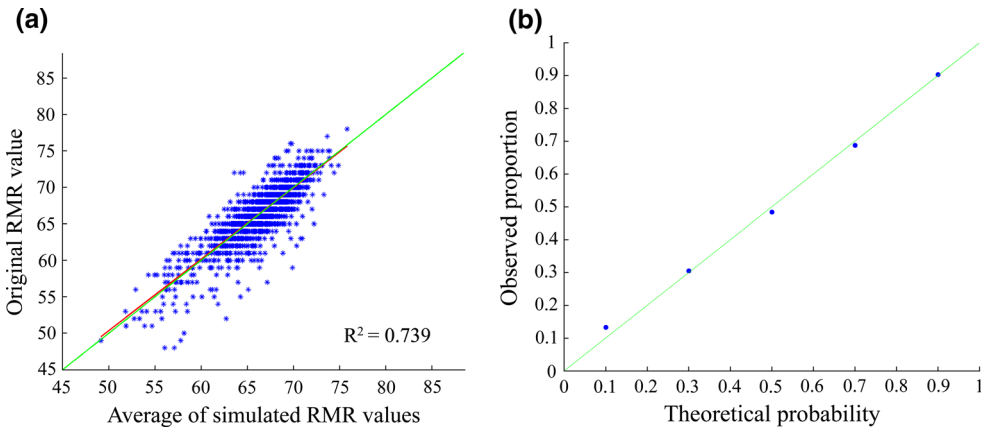

Fig. 3 Plots showing validation of: **a** the prediction capability; **b** uncertainty quantification

interval and 0 otherwise. This procedure is applied with p varying from 0.1 to 0.9. As a result (Fig. 3b), the observed proportion is close to the theoretical probability (points close to the diagonal line), indicating that the realizations accurately assess the uncertainty in the actual RMR values.

4 Conclusions

In this paper, a geostatistical approach for simulating RMR is presented, which considers the individual simulation of the underlying parameters constituting the RMR system and their summation to obtain the simulation of RMR. The split-sample validation technique shows good results in terms of prediction accuracy and measurement of uncertainty. The proposed approach provides information not only on RMR, but also on its underlying parameters, viewed as random fields measured on discrete quantitative scales, which is consistent with the nature of these parameters, which are ratings rather than variables defined on a continuous scale. Additionally, one can map the probability that RMR is higher or lower than a predefined threshold, or the dispersion of the simulated RMR values. These maps are useful for geotechnical analyses to quantify uncertainties and risks because they can assist in defining regions with contrasting quality and their probability of occurrence, or regions with higher uncertainty in the actual RMR values.

In future developments, the mapping of RMR and other parameters (like GSI and Q) complemented by the results of in situ and laboratory tests may be transformed into maps of the spatial distribution of geomechanical parameters. It is intended that these maps can be used to develop numerical models that explicitly consider the heterogeneities at all spatial scales, providing a more accurate understanding of the rock mass behavior than with traditional interpolation approaches.

Acknowledgments This research was supported by the Chilean Commission for Scientific and Technological Research (CONICYT),

through Projects CONICYT/FONDECYT/REGULAR/No 1130085 and CONICYT PIA Anillo ACT1407, and by Innova Chile CORFO 11IDL2-10630.

References

Armstrong M, Galli A, Beucher H, LeLoch G, Renard D, Doligez B, Eschard R, Geffroy F (2011) Plurigaussian simulations in geosciences, 2nd edn. Springer, Berlin **176pp**

Bieniawski ZT (1989) Engineering rock mass classifications. Wiley, New York **272 pp**

Chilès JP, Delfiner P (2012) Geostatistics: modeling spatial uncertainty. Wiley, New York **699 pp**

Deisman N, Khajeh M, Chalaturnyk RJ (2013) Using geological strength index (GSI) to model uncertainty in rock mass properties of coal for CBM/ECBM reservoir geomechanics. Int J Coal Geol 112:76–86

Egaña M, Ortiz J (2013) Assessment of RMR and its uncertainty by using geostatistical simulation in a mining project. J GeoEng 8(3):83–90

Emery X (2007) Simulation of geological domains using the plurigaussian model: new developments and computer programs. Comput Geosci 33(9):1189–1201

Emery X, Cornejo J (2010) Truncated Gaussian simulation of discrete-valued, ordinal coregionalized variables. Comput Geosci 36(10):1325–1338

Exadaktylos G, Stavropoulou M (2008) A specific upscaling theory of rock mass parameters exhibiting spatial variability: analytical relations and computational scheme. Int J Rock Mech Min Sci 45:1102–1125

Goovaerts P (2001) Geostatistical modeling of uncertainty in soil science. Geoderma 103:3–26

Jeon S, Hong C, You K (2009) Design of tunnel supporting system using geostatistical methods. In: Huang L (ed) Geotechnical aspects of underground construction in soft ground. pp 781–784

Lantuéjoul C (2002) Geostatistical simulation, models and algorithms. Springer, New York **256 pp**

Madani N, Asghari O (2013) Fault detection in 3D by sequential Gaussian simulation of rock quality designation (RQD). Arab J Geosci 12(10):3737–3747

Ozturk CA (2002) Geostatistical assessment of rock zones for tunneling. Tunn Undergr Space Technol 17:275–285

Ozturk CA, Simdi E (2014) Geostatistical investigation of geotechnical and constructional properties in Kadikoy-Kartal subway, Turkey. Tunn Undergr Space Technol 4:35–45

Rosenbaum MS, Rosen L, Gustafson G (1997) Probabilistic models for estimating lithology. Eng Geol 47:43–55

Ryu DW, Kim TK, Heo JS (2003) A study on geostatistical simulation technique for the uncertainty modeling of RMR. Tunn Undergr 13:87–99

Seokhoom O, Chung H, Kee Lee D (2004) Geostatistical integration of MT and boreholes data for RMR evaluation. Environ Geol 46:1070–1078

Stavropoulou M, Exadaktylos G, Saratsis G (2007) A combined three-dimensional geological-geostatistical-numerical model of underground excavations in rock. Int J Rock Mech Rock Eng 40(3):213–243